Deterministic correlations enhance synchronization in oscillator populations with heterogeneous coupling

Huajian Yu [1], Zhigang Zheng [2,*] and Can Xu [2,†]

[1] *School of Mathematical Sciences, Huaqiao University, Quanzhou 362021, China*

[2] *Institute of Systems Science and College of Information Science and Engineering, Huaqiao University, Xiamen 361021, China*

(Received 23 July 2023; accepted 11 October 2023; published 3 November 2023)

Synchronization is a critical phenomenon that displays a pivotal role in a wealth of dynamical processes ranging from natural to artificial systems. Here, we untangle the synchronization optimization in a system of globally coupled phase oscillators incorporating heterogeneous interactions encoded by the deterministic-random coupling. We uncover that, within the given restriction, the added deterministic correlations can profoundly enhance the synchronizability in comparison with the uncorrelated scenario. The critical points manifesting the onset of synchronization and desynchronization transitions, as well as the level of phase coherence, are significantly shaped by the increment of deterministic correlations. In particular, we provide an analytical treatment to properly ground the mechanism underlying synchronization enhancement and substantiate that the analytical predictions are in fair agreement with the numerical simulations. This study is a step forward in highlighting the importance of heterogeneous coupling among dynamical agents, which provides insights for control strategies of synchronization in complex systems.

DOI: 10.1103/PhysRevE.108.054203

I. INTRODUCTION

The emergence of spontaneous synchronization is a collective phenomenon that is pivotal in a wide range of physical, biological, chemical and engineered systems [1,2]. It represents a self-organizing dynamical process in which a population of interacting agents adjust their motion through the dissipative interactions, thereby achieving the coherence.

Coupled phase oscillator models, e.g., the Winfree and Kuramoto model, have proven to be useful tools for capturing and understanding synchronization during the last decades. In particular, these mathematical models elucidate synchronization at the onset of a nonequilibrium phase transition by reducing complex dynamics of limit cycles to phase equations of oscillators under the assumption of weak coupling [3].

In general, the interactions among dynamical units are assumed to be homogeneous, in which synchronization transitions are found to be continuous (second-order), i.e., the macroscopic order parameter characterizing the phase coherence of the system undergoes a supercritical bifurcation from the disordered (incoherent) state to an ordered (coherent) state, when the coupling strength exceeds a critical threshold [4–6].

However, recent studies have highlighted the importance of heterogeneous coupling, i.e., the interactions among oscillators are inhomogeneous (nonuniform). Beyond the uniform coupling, the heterogeneity underlies a number of realistic systems ranging from brain dynamics to social networks that has attracted ample attention [7–11]. Physically, it is more suitable to model dynamical systems by introducing the inhomogeneity into the coupling, where the responses of a unit to the interactions depend on the external or intrinsic diverse characteristics.

The systems of coupled oscillators incorporating the heterogeneity in the connection strength between interacting elements have revealed a plethora of dynamical phenomena. For instance, the networked heterogeneity with frequency-degree correlation triggers the onset of explosive synchronization [12–16], the quenched disorder of positive-negative coupling gives rise to a number of fascinating rhythmical states [17–22], the nonlocal coupling with long-range interactions leads to various chimera patterns [23–27], etc.

Most of the existing literature on the Kuramoto-like models has focused on exploring the effects of heterogeneous coupling on the emergence of various collective states. However, little attention has been paid to the synchronization capability itself. Namely, we are curious to see if the synchronizability gets affected by different arrangements of the heterogeneous coupling structures [28–31].

In this paper, we investigate synchronization dynamics in a system of heterogeneously coupled phase oscillators incorporating deterministic-random interactions. Specifically, we propose a strategy consisting of uniformly distributed couplings with different assignments, where a fraction of interactions are chosen to correlate with the oscillators' intrinsic frequencies while the remaining fraction remains random. The main issue addressed here is which type of coupling structure maximizes the synchronization capability of oscillators given a certain restriction. Intriguingly, we uncover that the introduced deterministic correlations can significantly enhance synchronization compared to the uncorrelated case. In particular, we reveal that there exists an optimal correlation in the subcritical regime, where the critical threshold corresponding to the onset of synchronization attains a minimum.

*zgzheng@hqu.edu.cn

†xucan@hqu.edu.cn

Moreover, we demonstrate that, after the onset, the increasing deterministic correlations are prone to favor synchronization, both by efficiently improving the degree of phase coherence and by prolonging its existing region. More importantly, we furnish an analytical treatment to comprehend the underlying mechanism behind synchronization optimization induced by the deterministic-random coupling.

The rest of this paper is organized as follows. In Sec. II, we introduce the dynamical model incorporating the deterministic-random coupling. In Sec. III, using the linear stability analysis, we obtain the forward critical coupling strength for the onset of synchronization that is significantly influenced by the correlation factor. In Sec. IV, we formulate a detailed self-consistent argument to account for synchronization optimization in various regions. Finally, discussion of the results and the conclusion are presented in Secs. V and VI, respectively.

II. DYNAMICAL MODEL

We consider a system of globally coupled phase oscillators that are governed by the following differential equations:

$$\dot{\theta}_i = \omega_i + \frac{K}{N}\alpha_i \sum_{j=1}^{N} \sin(\theta_j - \theta_i), \quad i = 1, \ldots, N. \tag{1}$$

Here, θ_i is the phase of the ith oscillator. $\{\omega_i\}$ are the natural frequencies of oscillators distributed according to a prescribed probability density function $g(\omega)$. $N \gg 1$ is the size of the system, and $K > 0$ represents the overall coupling strength of the system. Unless stated elsewhere, the natural frequencies are assumed to be evenly spaced over the interval $[-1, 1]$, i.e., $g(\omega)$ takes the uniform distribution of the form

$$g(\omega) = \begin{cases} \frac{1}{2} & |\omega| \leqslant 1, \\ 0 & \text{otherwise.} \end{cases} \tag{2}$$

As noted, the index-dependent factors $\{\alpha_i\}$ account for the inhomogeneous couplings among phase oscillators. Typically, there are several ways to endow the coupled system with the heterogeneity. One popular manner is to consider the factor α_i to be of the nonlocal coupling [32–35], where the coupling strength between a pair of oscillators decays over the distance. The most notable feature induced by the nonlocal coupling is the emergence of the chimera states [36–39], in which the identical oscillators separate into two distinct groups, one is phase-locked (synchronized) and the other is incoherent (desynchronized). Such remarkable phenomena occurring in systems of nonlocal coupling have attracted a great deal of theoretical and experimental interests over the past decades [40].

The nonlocal coupling arsing in diverse applications describes the interactions between the local (nearest-neighbor) and global (mean-field). Motivated by such a consideration, we here realize the set $\{\alpha_i\}$ by randomly extracting from the interval [0, 1] and then rearrange them according to their natural frequencies. Specifically, we set $\alpha_i = |\omega_i|$ for $|\omega_i| \leqslant C$, otherwise, $\{\alpha_i\}$ distribute uniformly in the range $(C, 1]$, $C \in [0, 1]$ serves as a tunable parameter reflecting the coupling-frequency correlation.

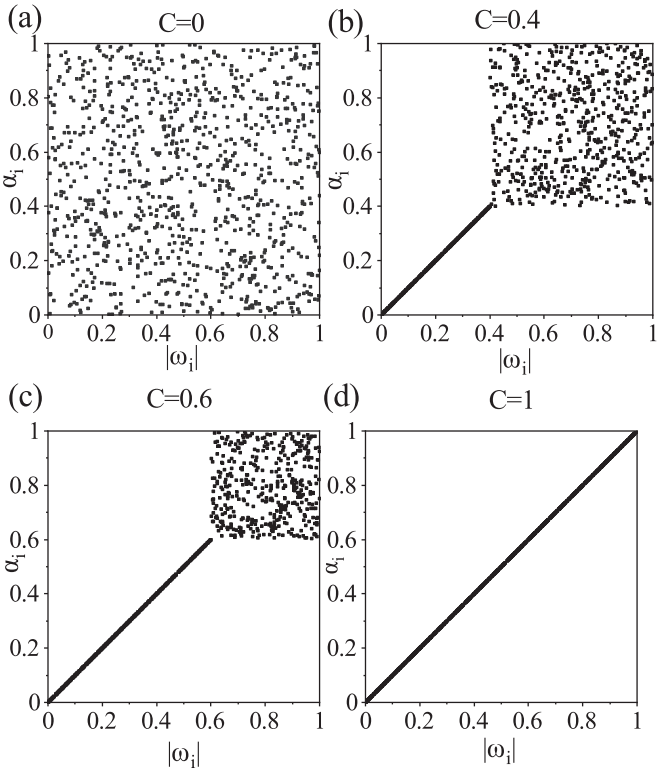

FIG. 1. The sketch maps of the coupling scheme DRC with different C. The vertical axis represents the index-depended factor α_i, and the horizontal axis is the absolute value of natural frequency $|\omega_i|$. Typically, the oscillator number is $N = 1000$.

Remarkably, when $C = 0$, $\{\alpha_i\}$ distribute uniformly in the interval [0, 1] that are totally uncorrelated with $\{\omega_i\}$. It represents a sort of quenched disorder of the system [41]. On the contrary, for the case $C = 1$, the two sets are completely correlated in a way such that $\alpha_i = |\omega_i|, \forall i = 1, \ldots, N$, which degenerates to the frequency-weighted coupling widely studied in previous works [42–46]. In the intermediate case $0 < C < 1$, the system is made up of two parts according to the magnitude of the natural frequencies with regard to C. Figure 1 illustrates the sketch map of the coupling scheme, in which different values of C distinguish with the different arrangements of the set $\{\alpha_i\}$. We henceforth refer to the dynamical model Eq. (1) as the deterministic-random coupling (DRC).

As stated, the coupling strategy introduced in Eq. (1) changes the coupling strength depending on the correlation factor C. Namely, the network is partitioned into two populations, and a positive correlation between the frequencies and couplings is set for a fraction of oscillators. We emphasize that the DRC serving as a peculiar coupling scheme has important applications in systems ranging from physics, biology to neuroscience. In particular, a number of fascinating collective states as well as a plethora intriguing dynamical phenomena are identified [47].

Most works have focused on revealing the inner relations between the structures and functions of the complex systems with DRC, such as the onset of explosive synchronization and various rhythm patterns. However, little attention has been

paid to explore the impacts of DRC on the synchronization capability. A natural question regarding the DRC is whether synchronization could be optimized by appropriately choosing the correlation factor C within a given restriction.

It is convenient to use a complex order parameter to monitor the globe coherence of the system, i.e.,

$$Z(t) = R(t)e^{i\Theta(t)} = \frac{1}{N}\sum_{j=1}^{N} e^{i\theta_j(t)}, \tag{3}$$

where $R(t) \in [0, 1]$ and $\Theta(t) \in [0, 2\pi)$ are, respectively, the amplitude and argument of the order parameter. Further, we restrict the analysis with two additional assumptions. First, N is assumed to be infinite (thermodynamic limit). In this regard, the joint distribution between α and ω takes the form

$$P(\alpha, \omega) = \delta(\alpha - |\omega|)H(C - |\omega|) + \frac{1}{1-C}H(|\omega| - C)H(\alpha - C)H(1 - \alpha), \tag{4}$$

where $\delta(\cdot)$ is the Dirac function and $H(\cdot)$ denotes the Heaviside function, i.e., $H(x) = 1$ for $x \geqslant 0$, otherwise $H(x) = 0$. Second, we are merely concerned with the stationary behaviors of the synchronized dynamics. In other words, $R(t)$ is assumed to be a constant in the long term and any nonstationary behaviors of the order parameter such as the standing waves are disregarded. In the following, we perform a detailed analysis to comprehend the underlying mechanism for synchronization optimization induced by the DRC both theoretically and numerically.

III. BELOW SYNCHRONIZATION: STABILITY ANALYSIS

To understand how the correlation factor C affects the critical point for the onset of synchronization, in this section, we are devoted to preforming a linear stability analysis of the asynchronous state. As we shall see below, the correlation factor C displays a nontrivial role in determining the forward critical point for synchronization transition.

A. Eigenvalue equation

To accomplish the stability analysis, it is convenient to describe Eq. (1) in the thermodynamic limit $N \to \infty$. In this representation, the microscopic state described by phase variables $\{\theta_i(t)\}$ is replaced by a macroscopic distribution function $\rho(\theta, \omega, \alpha, t)$ that obeys the continuity equation

$$\frac{\partial \rho}{\partial t} + \frac{\partial(\rho v)}{\partial \theta} = 0. \tag{5}$$

Here, $\rho(\theta, \omega, \alpha, t)d\theta$ accounts for the fraction of oscillators with the phases lying in the interval $(\theta, \theta + d\theta)$ at fixed parameters $\{\omega, \alpha, t\}$. It satisfies the normalization condition

$$\int_0^{2\pi} \rho(\theta, \omega, \alpha, t)d\theta = g(\omega)P(\alpha, \omega). \tag{6}$$

The velocity field v in Eq. (5) is given by

$$v(\theta, \omega, \alpha, t) = \omega + K\alpha\,\mathrm{Im}(Ze^{-i\theta}), \tag{7}$$

where $\mathrm{Im}(\cdot)$ denotes the imaginary part.

In the continuous limit, the macroscopic order parameter $Z(t)$ becomes

$$Z(t) = \int_0^1 d\alpha \int_{-1}^1 d\omega \int_0^{2\pi} e^{i\theta}\rho(\theta, \omega, \alpha, t)d\theta. \tag{8}$$

As for the asynchronous state, the oscillators run independently according to their natural frequencies. Roughly speaking, the instantaneous phases are scattered around the unity circle at time t and $Z(t) = 0$. Correspondingly, the distribution is

$$\rho_0(\theta, \omega, \alpha) = \frac{g(\omega)P(\alpha, \omega)}{2\pi}, \tag{9}$$

which is a trivial fixed point of Eq. (5).

Next, we linearize Eq. (5) around the fixed point Eq. (9). To this end, we introduce a small perturbation to Eq. (9), i.e.,

$$\rho(\theta, \omega, \alpha, t) = \rho_0(\theta, \omega, \alpha) + \varepsilon\eta(\theta, \omega, \alpha, t), \tag{10}$$

where $0 < \varepsilon \ll 1$ and $\eta(\theta, \omega, \alpha, t)$ denote the perturbed magnitude and function, respectively. The associated order parameter under the perturbation now becomes

$$Z[\eta] = \varepsilon \int_0^1 d\alpha \int_{-1}^1 d\omega \int_0^{2\pi} e^{i\theta}\eta(\theta, \omega, \alpha, t)d\theta, \tag{11}$$

which is proportional to the weak magnitude ε. Substituting Eqs. (9)–(11) into Eq. (5) and keeping the linear term of ε, we get

$$\frac{\partial \eta}{\partial t} = -\omega\frac{\partial \eta}{\partial \theta} + \frac{g(\omega)P(\alpha, \omega)}{2\pi}\alpha K\,\mathrm{Re}(e^{-i\theta}Z[\eta]), \tag{12}$$

where $\mathrm{Re}(\cdot)$ denotes the real part.

Recall that $\eta(\theta, \omega, \alpha, t)$ is a 2π-period function with respect to θ, it implies the Fourier series of the form

$$\eta(\theta, \omega, \alpha, t) = \sum_{n=-\infty}^{\infty} \eta_n(\omega, \alpha, t)e^{in\theta}. \tag{13}$$

We remark that $\eta_0 = 0$ due to the normalized condition Eq. (6) and $\eta_{-n} = \bar{\eta}_n$ owing to the real value of $\rho(\theta, \omega, \alpha, t)$, and "$\bar{\cdot}$" denotes the complex conjugate. Consequently, the perturbed order parameter reduces to

$$Z[\eta] = \varepsilon\, 2\pi \int_0^1 \int_{-1}^1 \eta_{-1}(\omega, \alpha, t)d\alpha d\omega. \tag{14}$$

According to Eq. (13), the analysis can be proceeded in each Fourier subspace independently. In doing so, Eq. (12) in the first Fourier subspace becomes

$$\frac{\partial \eta_1}{\partial t} = -i\omega\eta_1 + \frac{g(\omega)P(\alpha, \omega)}{2}\alpha K \int_0^1 \int_{-1}^1 \eta_1(\omega, \alpha, t)d\alpha d\omega. \tag{15}$$

Note that Eq. (15) consists in the fact that all the higher order Fourier terms have been disregarded, since they have no contribution to the order parameter. Therefore, the stability of the asynchronous state is determined by the linear evolution of the first Fourier mode only.

To proceed, let $\frac{\partial \eta_1}{\partial t} = \lambda \eta_1$ with λ being the eigenvalue of linearized dynamics, and then the eigenfunction is solved as

$$\eta_1(\omega, \alpha) = \frac{K\alpha}{2} \frac{g(\omega)P(\alpha, \omega)}{\lambda + i\omega} \int_0^1 \int_{-1}^1 \eta_1(\omega, \alpha) d\alpha d\omega. \quad (16)$$

Further, applying the integrals α and ω to both sides of Eq. (16), we arrive at the eigenvalue equation for λ yielding

$$\frac{1}{K} = \frac{1}{2} \int_0^1 d\alpha \int_{-1}^1 d\omega \frac{g(\omega)P(\alpha, \omega)\alpha}{\lambda + i\omega}. \quad (17)$$

B. Critical point and balanced equation

As above, the knowledge of the stability of the asynchronous state is controlled by the real parts of λ. Below, we focus on discussing the eigenvalue equation derived in Eq. (17) by taking into account the DRC.

Let $\lambda = x + iy$, with $x, y \in \mathbb{R}$ being the real and imaginary parts, respectively, and Eq. (17) can be transformed into the Cartesian coordinates as

$$\frac{1}{K} = \frac{1}{2} \int_0^1 d\alpha \int_{-1}^1 d\omega \frac{xg(\omega)P(\alpha, \omega)\alpha}{x^2 + (y + \omega)^2}, \quad (18)$$

$$0 = \frac{1}{2} \int_0^1 d\alpha \int_{-1}^1 d\omega \frac{(y + \omega)g(\omega)P(\alpha, \omega)\alpha}{x^2 + (y + \omega)^2}. \quad (19)$$

On the one hand, for a sufficiently small value of K, there are no roots to Eqs. (18) and (19). This is because $K^{-1} \to \infty$, while the right hand side of Eq. (18) remains bounded for any values of (x, y). Hence, the eigenvalue λ is absent for small K[48]. On the other hand, x is always larger than zero due to $K > 0$ in Eq. (18). The nonzero roots appear once K exceeds a threshold implying the instability of the asynchronous state. Therefore, the critical point K_f corresponding to the onset of synchronization is obtained by imposing the limits $x \to 0^+, y \to \Omega$.

Considering the specific forms of $g(\omega)$ and $P(\alpha, \omega)$, Eq. (18) reduces to

$$\begin{aligned}\frac{1}{K} &= \frac{1}{4} \int_0^1 d\alpha \int_{-1}^1 d\omega \frac{\delta(\alpha - |\omega|)\alpha x}{x^2 + (y + \omega)^2} \\ &\quad + \frac{1}{4(1 - C)} \int_C^1 d\alpha \int_{C<|\omega|<1} d\omega \frac{\alpha x}{x^2 + (y + \omega)^2} \\ &= \frac{1}{4} \int_{-C}^{C} \frac{\delta(\alpha - |\omega|)x}{x^2 + (y + \omega)^2} d\omega \\ &\quad + \frac{1 + C}{8} \int_{C<|\omega|<1} \frac{x}{x^2 + (y + \omega)^2} d\omega. \end{aligned} \quad (20)$$

At the critical point K_f, we have

$$\frac{1}{K_f} = \frac{\pi}{4} |\Omega| H(C - |\Omega|) + \frac{1 + C}{8} \pi H(|\Omega| - C), \quad (21)$$

where we have used the identity limit $x \to 0^+$,

$$\frac{x}{x^2 + (\Omega + \omega)^2} = \pi \delta(\Omega + \omega). \quad (22)$$

Therefore, the critical point K_f is obtained as

$$K_f = \frac{8}{2\pi |\Omega| H(C - |\Omega|) + (1 + C)\pi H(|\Omega| - C)}, \quad (23)$$

and the critical frequency Ω satisfies the balanced equation

$$0 = \text{P.V.} \left(\int_{-C}^{C} \frac{2|\omega|}{\omega + \Omega} d\omega + (1 + C) \int_{C<|\omega|<1} \frac{1}{\omega + \Omega} d\omega \right), \quad (24)$$

where P.V. denotes the Cauchy principal value integral.

Equation (23) indicates that the critical point K_f depends on the critical frequency Ω, as well as the correlation factor C. To obtain insights for K_f, the balanced equation Eq. (24) should be discussed in three different scenarios.

Case I, $0 \leqslant |\Omega| < C$, the first term at right-hand side of Eq. (24) diverges that should be integrated in the sense of principal value. Straightforward calculations yield

$$0 = -2\Omega \ln \frac{C^2 - \Omega^2}{\Omega^2} + (1 + C) \ln \frac{(\Omega + 1)(\Omega - C)}{(\Omega - 1)(\Omega + C)}. \quad (25)$$

Case II, $C \leqslant |\Omega| < 1$, the second term at right-hand side of Eq. (24) becomes singular and should be performed in the principal-valued sense, which is

$$0 = -2\Omega \ln \frac{\Omega^2 - C^2}{\Omega^2} + (1 + C) \ln \frac{(\Omega + 1)(C - \Omega)}{(\Omega - 1)(\Omega + C)}. \quad (26)$$

Case III, $|\Omega| \geqslant 1$, both terms at right-hand side of Eq. (24) are bounded, and then the integral can be preformed over the whole interval, which becomes

$$0 = -2\Omega \ln \frac{\Omega^2 - C^2}{\Omega^2} + (1 + C) \ln \frac{(\Omega + 1)(\Omega - C)}{(\Omega - 1)(\Omega + C)}. \quad (27)$$

Taken together, the balanced equations, Eqs. (25)–(27), can be expressed in a unified form, i.e.,

$$0 = -2\Omega \ln \frac{|\Omega^2 - C^2|}{\Omega^2} + (1 + C) \ln \left| \frac{(\Omega + 1)(\Omega - C)}{(\Omega - 1)(\Omega + C)} \right|. \quad (28)$$

Based on the analysis above, we conclude that the correlation factor C determines the critical frequency Ω in terms of Eq. (28), which in turn locates the critical point K_f via Eq. (23). It should be pointed out that there might exist several roots of Ω to Eq. (28) implying the multivalues of the critical point. Physically, K_f takes the minimum value corresponding to the foremost instability of the incoherent state.

C. Perturbation analysis

In general, it is difficult to get explicit expressions for the critical frequency Ω and the forward critical point K_f as a function of C. Nevertheless, to gain some intuition about the results obtained above, we next utilize the perturbation theory to obtain the asymptotic behaviors of Ω and K_f near $C = 0$, i.e., the scaling behaviors of Ω and K_f near $C = 0$.

Notice that, for the completely uncorrelated case with $C = 0$, it can be easily verified that $\Omega = 0$ is the only solution to Eq. (28). To proceed, let

$$C = 0 + \varepsilon (0 < \varepsilon \ll 1), \quad (29)$$

and we assume that

$$\Omega = 0 + \varepsilon^\beta \Omega_1 (0 < |\Omega_1| < \infty), \quad (30)$$

in which the scaling exponent β as well as the coefficient Ω_1 are yet unknowns to be determined.

Before going further, we stress that if $|\Omega| < C = \varepsilon$, then $K_f \sim |\Omega|^{-1}$, which is singular for $\varepsilon \to 0$. Hence, we rule out this case and assume that $|\Omega| > C$. On this backdrop, the perturbed analysis is based on the balanced equation Eq. (26).

Substituting Eqs. (29) and (30) into Eq. (26), we get the perturbed balanced equation

$$0 = S(\varepsilon, \Omega_1) + Q(\varepsilon, \Omega_1), \tag{31}$$

with

$$S(\varepsilon, \Omega_1) = -2\varepsilon^{\beta}\Omega_1 \ln\left(1 - \frac{\varepsilon^{2(1-\beta)}}{\Omega_1^2}\right) \tag{32}$$

and

$$Q(\varepsilon, \Omega_1) = (1+\varepsilon)\ln\frac{\varepsilon^{\beta}\left(-\Omega_1^2\right) + \varepsilon^{1-\beta} + \varepsilon\Omega_1 - \Omega_1}{\varepsilon^{\beta}\Omega_1^2 - \varepsilon^{1-\beta} + \varepsilon\Omega_1 - \Omega_1}. \tag{33}$$

Observe that $S(\varepsilon, \Omega_1)$ can be expressed in terms of the Taylor series, that is

$$S(\varepsilon, \Omega_1) \sim \varepsilon^{2-\beta}\frac{2}{\Omega_1}. \tag{34}$$

Since $|\Omega| > C$, we must have $0 < \beta \leqslant 1$, and Eq. (34) turns out to be a higher order term of ε. Below, we distinguish with three different cases of β to discuss the second term $Q(\varepsilon, \Omega_1)$.

Case I, $0 < \beta < \frac{1}{2}$, we remark that ε^{β} appearing in $Q(\varepsilon, \Omega_1)$ is a leading term. As a result, $\varepsilon^{1-\beta}$ and ε become higher-order terms compared with ε^{β} that should be neglected. We thus have

$$\begin{aligned} Q(\varepsilon, \Omega_1) &= (1+\varepsilon)\ln\frac{\varepsilon^{\beta}\left(-\Omega_1^2\right) - \Omega_1}{\varepsilon^{\beta}\Omega_1^2 - \Omega_1} \\ &\sim \varepsilon^{\beta}(2\Omega_1) + \varepsilon^{\beta+1}(2\Omega_1). \end{aligned} \tag{35}$$

Case II, $\frac{1}{2} < \beta < 1$, $\varepsilon^{1-\beta}$ automatically becomes a dominant term compared to ε^{β} and ε, and we have

$$\begin{aligned} Q(\varepsilon, \Omega_1) &= (1+\varepsilon)\ln\frac{\varepsilon^{1-\beta} - \Omega_1}{-\varepsilon^{1-\beta} - \Omega_1} \\ &\sim -\varepsilon^{1-\beta}\left(\frac{2}{\Omega_1}\right) - \varepsilon^{2-\beta}\left(\frac{2}{\Omega_1}\right). \end{aligned} \tag{36}$$

Case III, $\beta = \frac{1}{2}$, $\varepsilon^{\beta} = \varepsilon^{1-\beta}$ and the term ε should be ignored, which leads to

$$\begin{aligned} Q(\varepsilon, \Omega_1) &= (1+\varepsilon)\ln\frac{\sqrt{\varepsilon}(1-\Omega_1^2) - \Omega_1}{\sqrt{\varepsilon}\left(\Omega_1^2 - 1\right) - \Omega_1} \\ &\sim \sqrt{\varepsilon}\left(-\frac{2}{\Omega_1} + 2\Omega_1\right) + \sqrt{\varepsilon^3}\left(-\frac{2}{\Omega_1} + 2\Omega_1\right). \end{aligned} \tag{37}$$

The basic idea behind the perturbed analysis demands that the leading terms of ε in $S(\varepsilon, \Omega_1)$ and $Q(\varepsilon, \Omega_1)$ should cancel each other out, which hints that $\Omega_1 = 0$ for case I and $\Omega_1 = \pm\infty$ for case II. Apparently, this two conditions violate the presuppositions mentioned in Eq. (30). We claim that only case III with $\beta = \frac{1}{2}$ is admittable, implying that $\Omega_1 = \pm 1$. Therefore, the scaling behaviors for the critical points are

$$K_f \sim \frac{8}{\pi(1+C)}, \quad \Omega \sim \pm\sqrt{C}(0 < C \ll 1), \tag{38}$$

which are shown in Fig. 2.

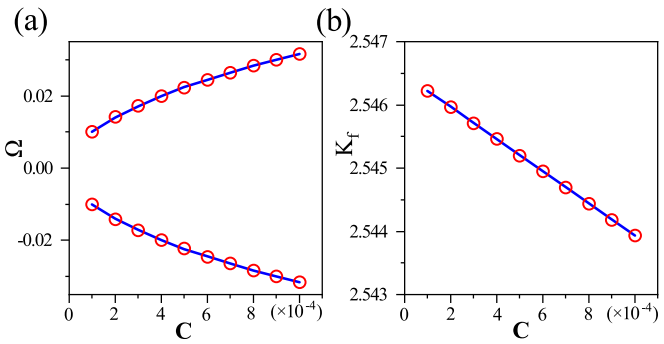

FIG. 2. The scaling behaviors of the critical points. (a) Ω vs C, the blue solid line corresponds to Eq. (38) and the red circles are solutions to Eq. (30). (b) K_f vs C, the blue solid line is given by Eq. (38) and the red circles are obtain by numerically simulating Eq. (1) with $N = 50\,000$.

D. Discussions

To summarize, Fig. 3 plots the forward critical point K_f as a function of the correlation factor C, in which the solid line is the theoretical prediction obtained by Eqs. (23)–(28) and the circles are corresponding numerical simulations of Eq. (1). We concisely state the findings as follows:

It can be shown from Fig. 3 that the plot K_f exhibits a discontinuous parabolic-like shape with respect to C. Specifically, K_f is decreasing for $0 \leqslant C < C^{\star} \approx 0.75$, after that it jumps discontinuously to a value and then gradually increases until $C = 1$. The mathematical consequence of the discontinuity of K_f at $C^{\star}$ can be understood as follows. We emphasize that it stems from the discontinuity of the Heaviside function in Eq. (23). First, when $0 \leqslant C < C^{\star}$, numerical solutions

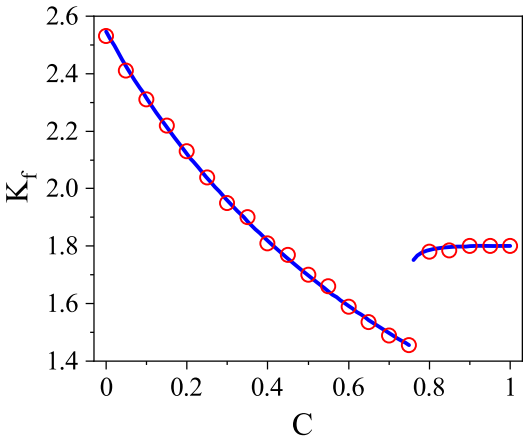

FIG. 3. The forward critical point K_f vs the correlation factor C. The blue solid line represents the theoretical prediction by Eq. (23) and the red circles are numerical simulations with $N = 50\,000$.

of Eq. (28) reveal that $|\Omega| > C$, and hence only the term $H(|\Omega| - C)$ is valid. In this region, $K_f = 8/\pi(1 + C)$, which generalizes the result obtained by the perturbed analysis [see Eq. (38)]. Second, once $C > C^\star$, the solutions of Eq. (28) indicate that $|\Omega| < C$, such as $\Omega \to \pm\sqrt{2}/2$ for $C \to 1$. Thus, only the term $H(C - |\Omega|)$ is effective. For that matter, $K_f = 4/\pi|\Omega|$. In a addition, the gradual increment of $|\Omega|$ with respect to C results in the saturation of K_f for $C > C^\star$.

The conclusion we can draw from the stability analysis is that the correlation factor has a significant influence on the threshold for synchronization transition. When $C = 0$, the frequency and coupling are totally uncorrelated, at which the critical point corresponding to the onset of synchronization attains the maximum, i.e., $K_f = 8/\pi$. However, if the deterministic correlation is introduced ($C > 0$), then K_f gets decreased and the deterministic correlation is prone to promote the onset of synchronization. Strikingly, it is found that there exists a critical correlation factor, at which K_f attains the minimum. Finally, for $C^\star < C \approx 1$, K_f tends to a constant, i.e., $K_f \approx 4\sqrt{2}/\pi$. The overall effect of the deterministic correlation is to render the synchronization transition easier.

IV. ABOVE SYNCHRONIZATION: SELF-CONSISTENT ARGUMENT

In the proceeding section, the forward critical point K_f was obtained using the linear stability analysis. It was revealed that deterministic correlations favor synchronization transition. In this section, we continue to explore the effects of the correlations aiming at uncovering the underlying mechanism for synchronization optimization induced by DRC. In doing so, we resort to the self-consistent approach that is capable of capturing the stationary behaviors of the equilibrium states in the long-time limit.

A. Self-consistent equations

We first write the mean-field form of Eq. (1) as

$$\dot{\theta} = \omega + \alpha q \sin(\Theta - \theta), \tag{39}$$

where $q = KR \geqslant 0$ is introduced to ease notation, and the index i has been dropped in the limit $N \to \infty$. By equilibrium sates, it means that the order parameter tends to a constant and the average phase rotates uniformly on the unit circle, i.e., $R(t) = R$ and $\Theta(t) = \Omega t + \Omega_0$. Furthermore, the dynamical system possesses rotational and reflectional symmetries leading to $\Theta(t) = 0$ by shifting initial conditions and going into a rotating frame. With this, the mean field equation Eq. (39) is simplified as

$$\dot{\theta} = \omega - \alpha q \sin(\theta). \tag{40}$$

Clearly, the system can be divided into two distinct clusters according to the relative magnitude $|\omega|/\alpha q$. For the case $|\omega| < \alpha q$, the velocity $v = 0$ and the oscillators are phase-locked with

$$\sin\theta_\star = \frac{\omega}{\alpha q}, \quad \cos\theta_\star = \sqrt{1 - \frac{\omega^2}{\alpha^2 q^2}}. \tag{41}$$

The distribution formed by the locked oscillators is expressed as

$$\rho_l(\theta, \omega, \alpha) = g(\omega)P(\alpha, \omega)\delta(\theta - \theta_\star). \tag{42}$$

In contrast, for the case $|\omega| > \alpha q$, the velocity $v \neq 0$ and the oscillators behave as drifters, which can never be entrained by the mean field. Correspondingly, the stationary distribution obtained from Eq. (5) is given by

$$\rho_d(\theta, \omega, \alpha) = g(\omega)P(\alpha, \omega)\frac{\sqrt{\omega^2 - \alpha^2 q^2}}{2\pi|\omega - q\alpha\sin\theta|}. \tag{43}$$

Turning to the order parameter $Z(t)$, it can be expressed as

$$Z = \langle e^{i\theta}\rangle_l + \langle e^{i\theta}\rangle_d, \tag{44}$$

where $\langle\cdot\rangle_{l,d}$ denote the average over the locked and drifting populations, respectively. Furthermore, straightforward calculations yield $\langle e^{i\theta}\rangle_d = \langle\sin\theta_\star\rangle_l = 0$ due to the symmetry of the system. Keeping all these in mind, the expression for the order parameter is

$$R = \int_0^1 d\alpha \int_{-1}^1 d\omega g(\omega)P(\alpha, \omega)\sqrt{1 - \frac{\omega^2}{\alpha^2 q^2}}. \tag{45}$$

Considering the definition $g(\omega)$ and $P(\alpha, \omega)$, the self-consistent equation, Eq. (45), can be reformulated into a simple form

$$\frac{1}{K} = F(q), \tag{46}$$

with the characteristic function being

$$F(q) = \frac{1}{2q}\int_0^1 d\alpha \int_{-1}^1 d\omega\Big[\delta(\alpha - |\omega|)H(C - |\omega|) + \frac{1}{1 - C}H(|\omega| - C)H(\alpha - C)H(1 - \alpha)\Big] \times\sqrt{1 - \frac{\omega^2}{\alpha^2 q^2}}. \tag{47}$$

The self-consistent equations Eqs. (46) and (47) provide a general framework for delineating the stationary synchronized dynamics with DRC. In what follows, we discuss various scenarios to establish analytic formulas for $F(q)$.

Before proceeding, several symbols are defined to simplify notation. Namely, $\Delta = 1 - \omega^2/\alpha^2 q^2$, $I_{\alpha,\omega}$ denote the integral intervals of α and ω, respectively. "$a \Rightarrow b$" represents the equivalence between a and b. $\emptyset$ denotes the empty set.

B. $0 \leqslant q < 1$

Notice that the phase-locked condition requires that $|\omega| < \alpha q$. Since $\alpha \in [0, 1]$, for the case $0 \leqslant q < 1$, we always have $\alpha q \in [0, 1)$. So, the characteristic function $F(q)$ in this region becomes

$$F_{q<1} = \frac{1}{2q}\int_0^1 d\alpha \int_{-\alpha q}^{\alpha q} d\omega P(\alpha, \omega)\sqrt{\Delta}. \tag{48}$$

Because $P(\alpha, \omega)$ consists of two parts, it is convenient to discuss Eq. (48) by dividing it into two different terms.

1. The first term

The first term of Eq. (48) reads

$$F_{q<1,(1)} = \frac{1}{2q}\int_0^1 d\alpha \int_{-\alpha q}^{\alpha q} d\omega \delta(\alpha - |\omega|)H(C-|\omega|)\sqrt{\Delta} = \frac{1}{q}\int_0^1 d\alpha \int_0^{\alpha q} d\omega \delta(\alpha - |\omega|)H(C-\omega)\sqrt{\Delta}, \quad (49)$$

where we have used the evenness of the integral function of ω.

Observe that the Heaviside function $H(C-\omega)$ demands that $0 \leqslant \omega < C$. Hence, we must distinguish with two cases $\alpha q < C$ and $\alpha q > C$, respectively. For the first scenario, the integral Eq. (49) becomes

$$F^{\alpha q<C}_{q<1,(1)} = \frac{1}{q}\int_0^1 d\alpha \int_0^{\alpha q} d\omega \delta(\alpha-\omega)\sqrt{\Delta}. \quad (50)$$

Recall that the integral variable ω in Eq. (50) varies from 0 to αq, which is strictly less than α (since $0 \leqslant q < 1$). Accordingly, the Dirac function $\delta(\alpha-\omega)$ is always zero over the integral range I_ω, which results in

$$F^{\alpha q<C}_{q<1,(1)} = 0. \quad (51)$$

For the second scenario with $\alpha q > C$, $I_\omega = (0, C)$ and the integral Eq. (49) becomes

$$F^{\alpha q>C}_{q<1,(1)} = \frac{1}{q}\int_0^1 d\alpha \int_0^{C} d\omega \delta(\alpha-\omega)\sqrt{\Delta}. \quad (52)$$

We note that $\alpha q > C \Rightarrow \alpha > \frac{C}{q}$. First, if $q < C$, then $\alpha > 1$, which should be ruled out. Second, if $C < q < 1$, then the integral above is

$$F^{\alpha q>C, q>C}_{q<1,(1)} = \frac{1}{q}\int_{\frac{C}{q}}^1 d\alpha \int_0^{C} d\omega \delta(\alpha-\omega)\sqrt{\Delta} = 0. \quad (53)$$

This is because $I_\omega = (0, C)$ and $I_\alpha = (\frac{C}{q}, 1)$. Apparently, these two intervals can never overlap, and thus the Dirac function $\delta(\alpha-\omega)$ is always zero.

Taken together, for $0 \leqslant q < 1$, the first term in the characteristic function $F(q)$ is

$$F_{q<1,(1)} \equiv 0. \quad (54)$$

2. The Second term

As for the second term, the characteristic function $F(q)$ becomes

$$F_{q<1,(2)} = \frac{1}{q(1-C)}\int_C^1 d\alpha \int_0^{\alpha q} d\omega H(\omega - C)\sqrt{\Delta}. \quad (55)$$

The Heaviside function $H(\omega - C)$ requires that $\omega > C$ so the case $\alpha q < C$ should be disregarded, and Eq. (55) degenerates to

$$F^{\alpha q>C}_{q<1,(2)} = \frac{1}{q(1-C)}\int_{\frac{C}{q}}^1 d\alpha \int_C^{\alpha q} d\omega \sqrt{\Delta}. \quad (56)$$

Note that we have used the fact in Eq. (56) that $\alpha q > C \Rightarrow \alpha > \frac{C}{q} > C$. Remarkably, for $q < C$, the integral range for α in Eq. (56) vanishes and should be ruled out. Hence, only the case $q > C$ is admittable, which yields

$$F^{\alpha q>C, q>C}_{q<1,(2)} = \frac{1}{q(1-C)}\int_{\frac{C}{q}}^1 d\alpha \int_C^{\alpha q} d\omega \sqrt{\Delta}. \quad (57)$$

Combining the results above, the characteristic function $F(q)$ in the region $0 \leqslant q < 1$ begets

$$F_{C<q<1} = \frac{3C\sqrt{-C^2+q^2} - (2C^2+q^2)\arccos\frac{C}{q}}{4(-1+C)q^2}. \quad (58)$$

C. $q > 1$

We next turn to the case $q > 1$, in which $\alpha q \in [0, +\infty)$ and the discussion about the characteristic function $F(q)$ becomes more intricate compared to the case $q < 1$. For convenience, the integral restricted in this region is rewritten as

$$F_{q>1} = \frac{1}{2q}\int_0^1 d\alpha \int_{-1}^1 d\omega P(\alpha,\omega)\sqrt{\Delta}. \quad (59)$$

To guarantee the positiveness of Δ, one has $I_\omega = (-\alpha q, \alpha q)$. Likewise, we must distinguish with two cases $\alpha q < 1$ and $\alpha q > 1$, respectively. Namely,

$$F_{q>1,\alpha q<1} = \frac{1}{q}\int_0^{\frac{1}{q}} d\alpha \int_0^{\alpha q} d\omega P(\alpha,\omega)\sqrt{\Delta}, \quad (60)$$

in which $\alpha q < 1 \Rightarrow \alpha < \frac{1}{q} < 1$, and

$$F_{q>1,\alpha q>1} = \frac{1}{q}\int_{\frac{1}{q}}^1 d\alpha \int_0^1 d\omega P(\alpha,\omega)\sqrt{\Delta}. \quad (61)$$

As before, we proceed with the analysis by dividing the integrals Eqs. (60) and (61) into two terms, respectively.

1. The first term ($\alpha q < 1$)

The first term with $\alpha q < 1$ is expressed as

$$F_{q>1,\alpha q<1,(1)} = \frac{1}{q}\int_0^{\frac{1}{q}} d\alpha \int_0^{\alpha q} d\omega \delta(\alpha-\omega)H(C-\omega)\sqrt{\Delta}. \quad (62)$$

First, we suppose that $\alpha q < C \Rightarrow \alpha < \frac{C}{q} < \frac{1}{q}$. In addition, $0 < \omega < \alpha q < C$ implies that $H(C-\omega) \equiv 1$, and $q > 1$ means that $I_\alpha \subset I_\omega$. Therefore, Eq. (62) with $\alpha q < C$ reduces to

$$F^{\alpha q<C}_{q>1,\alpha q<1,(1)} = \frac{1}{q}\int_0^{\frac{C}{q}} d\alpha \sqrt{1-q^{-2}} = Cq^{-2}\sqrt{1-q^{-2}} \quad (63)$$

Second, we assume that $\alpha q > C \Rightarrow \alpha > \frac{C}{q} (< \frac{1}{q})$ and $I_\omega = (0, C)$, which satisfies $H(C-\omega) = 1$. Then we have

$$F^{\alpha q>C}_{q>1,\alpha q<1,(1)} = \frac{1}{q}\int_{\frac{C}{q}}^{\frac{1}{q}} d\alpha \int_0^{C} d\omega \delta(\alpha-\omega)\sqrt{\Delta}. \quad (64)$$

The next step is to discuss the Dirac function. Observe that $\frac{C}{q} < C$. Further, if $\frac{1}{q} < C \Rightarrow q > \frac{1}{C}$, then we have $I_\alpha \subset I_\omega$,

which yields

$$F^{\alpha q>C,q>C^{-1}}_{q>1,\alpha q<1,(1)} = \frac{1}{q}\int_{\frac{C}{q}}^{\frac{1}{q}} d\alpha\sqrt{1-q^{-2}} = (1-C)q^{-2}\sqrt{1-q^{-2}}. \quad (65)$$

If $\frac{1}{q} > C \Rightarrow q < \frac{1}{C}$, then the integral range for α should be split into two subintervals, i.e., $I_\alpha = (\frac{C}{q}, C) \cup (C, \frac{1}{q})$. Obviously, $I_\omega \cap (C, \frac{1}{q}) = \emptyset$, we get

$$F^{\alpha q>C,q<C^{-1}}_{q>1,\alpha q<1,(1)} = \frac{1}{q}\int_{\frac{C}{q}}^{C} d\alpha\sqrt{1-q^{-2}} = C(q-1)q^{-2}\sqrt{1-q^{-2}}. \quad (66)$$

2. *The second term* ($\alpha q < 1$)

The second term with $\alpha q < 1$ is expressed as

$$F_{q>1,\alpha q<1,(2)} = \frac{1}{q(1-C)}\int_0^{\frac{1}{q}} d\alpha \int_0^{\alpha q} d\omega H(\omega - C) \times H(\alpha - C)\sqrt{\Delta}. \quad (67)$$

Notice that, for $\frac{1}{q} < C \Rightarrow q > \frac{1}{C}$, we must have $H(\alpha - C) \equiv 0$ for $\alpha \in I_\alpha$, and which yields

$$F^{q>C^{-1}}_{q>1,\alpha q<1,(2)} = 0. \quad (68)$$

On the contrary, for $q < \frac{1}{C}$, we have $I_\alpha = (C, \frac{1}{q})$ to ensure that $H(\alpha - C) = 1$. Furthermore, if $\alpha q < C \Rightarrow H(\omega - C) \equiv 0$ for $\omega \in I_\omega$, then we thus have

$$F^{q<C^{-1},\alpha q<C}_{q>1,\alpha q<1,(2)} = 0. \quad (69)$$

However, if $\alpha q > C$, $I_\omega = (C, \alpha q)$ to ensure $H(\omega - C) = 1$, then we get (see the Appendix)

$$F^{q<C^{-1},\alpha q>C}_{q>1,\alpha q<1,(2)} = \frac{1}{q(1-C)}\int_C^{\frac{1}{q}} d\alpha \int_C^{\alpha q} d\omega\sqrt{\Delta}. \quad (70)$$

Up to now, we have finished the first step for the derivation of $F(q)$ with $q > 1$ and $\alpha q < 1$. In the following, we calculate $F(q)$ with $q > 1$ and $\alpha q > 1$.

3. *The first term* ($\alpha q > 1$)

In this region, $\alpha q > 1 \Rightarrow \alpha > \frac{1}{q} \Rightarrow I_\alpha = (\frac{1}{q}, 1)$. The first term corresponds to

$$F_{q>1,\alpha q>1,(1)} = \frac{1}{q}\int_{\frac{1}{q}}^{1} d\alpha \int_0^C d\omega\delta(\alpha - \omega)\sqrt{\Delta}, \quad (71)$$

where we have used $I_\omega = (0, C) \subset (0, 1)$ to account for $H(C - \omega)$.

Likewise, if $q < C^{-1}$, then $I_\alpha \cap I_\omega = \emptyset$, which implies

$$F^{q<C^{-1}}_{q>1,\alpha q>1,(1)} = 0. \quad (72)$$

In contrast, $q > C^{-1}$, $I_\alpha = (\frac{1}{q}, C) \cup (C, 1)$, which results in $(\frac{1}{q}, C) \subset I_\omega$ and $I_\omega \cap (C, 1) = \emptyset$, we obtain

$$F^{q>C^{-1}}_{q>1,\alpha q>1,(1)} = \frac{1}{q}\int_{\frac{1}{q}}^{C} d\alpha\sqrt{1-q^{-2}} = (qC-1)q^{-2}\sqrt{1-q^{-2}}. \quad (73)$$

4. *The second term* ($\alpha q > 1$)

In this region, $I_\omega = (C, 1)$ and we have

$$F_{q>1,\alpha q>1,(2)} = \frac{1}{q(1-C)}\int_{\frac{1}{q}}^{1} d\alpha \int_C^1 d\omega H(\alpha - C)\sqrt{\Delta}. \quad (74)$$

Also, we assume that $\frac{1}{q} > C \Rightarrow q < C^{-1}$, which hints that $\alpha > C$ always holds $\Rightarrow H(\alpha - C) \equiv 1$ for $\alpha \in I_\alpha$. After tedious calculations, we get (see the Appendix)

$$F^{q<C^{-1}}_{q>1,\alpha q>1,(2)} = \frac{1}{q(1-C)}\int_{\frac{1}{q}}^{1} d\alpha \int_C^1 d\omega\sqrt{\Delta}. \quad (75)$$

However, for $\frac{1}{q} < C \Rightarrow q > C^{-1}$, I_α turns out to be $(C, 1)$. We have that

$$F^{q>C^{-1}}_{q>1,\alpha q>1,(2)} = \frac{1}{q(1-C)}\int_C^{1} d\alpha \int_C^1 d\omega\sqrt{\Delta}, \quad (76)$$

and the detailed results are included in the Appendix.

Taken together, the characteristic function $F(q)$ in the region $q > 1$ is summarized as

$$F_{1<q<C^{-1}} = F^{\alpha q<C}_{q>1,\alpha q<1,(1)} + F^{\alpha q>C,q<C^{-1}}_{q>1,\alpha q<1,(1)} + F^{q<C^{-1},\alpha q<C}_{q>1,\alpha q<1,(2)} + F^{q<C^{-1},\alpha q>C}_{q>1,\alpha q<1,(2)} + F^{q<C^{-1}}_{q>1,\alpha q>1,(1)} + F^{q<C^{-1}}_{q>1,\alpha q>1,(2)} \quad (77)$$

and

$$F_{q>C^{-1}} = F^{\alpha q<C}_{q>1,\alpha q<1,(1)} + F^{\alpha q>C,q>C^{-1}}_{q>1,\alpha q<1,(1)} + F^{q>C^{-1}}_{q>1,\alpha q<1,(2)} + F^{q>C^{-1}}_{q>1,\alpha q>1,(1)} + F^{q>C^{-1}}_{q>1,\alpha q>1,(2)}, \quad (78)$$

which completes the derivation of $F(q)$ in both regions.

D. Discussions

Combining Eqs. (77) and (78) with Eq. (58), the results of $F(q)$ are condensed in Fig. 4 for typical values of C. It is observed that the function $F(q)$ is defined in four regions, respectively. Precisely, $F(q)$ is undefined for $q \in [0, C)$ and the self-consistent argument is not applicable. For $q \in [C, 1)$, the function $F(q)$ is expressed by Eq. (58) which is nondecreasing. While for $q \in [1, C^{-1}) \cup (C^{-1}, \infty)$, the function $F(q)$ are respectively given by Eqs. (77) and (78), whose monotonicity strongly relies on the correlation factor C. We here exemplify two special cases to showcase the characteristic function $F(q)$, i.e., $C = 0$ and $C = 1$. In the situation $C = 0$, the intrinsic frequencies and distributed couplings are totally uncorrelated, such that $F(q) = \pi/8$ for $q \in [0, 1)$ that is a constant,

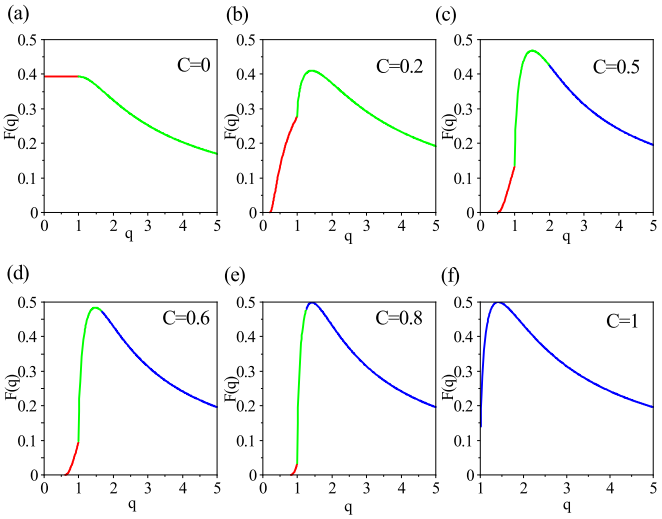

FIG. 4. The characteristic function $F(q)$ vs q with typical values of C. The red, green and blue solid lines represent the values of $F(q)$ in the intervals $[C, 1)$, $[1, C^{-1})$ and $[C^{-1}, 5]$, respectively.

and $F(q) = (6\sqrt{q^2-1} + 2q^2 \operatorname{arccsc} q - 4 \operatorname{arcsec} q)/8q^2$ for $q \geqslant 1$. In the scenario $C = 1$, the random frequencies and couplings are completely deterministically correlated in a way, such that $F(q)$ is vastly simplified as $F(q) = q^{-1}\sqrt{1-q^{-2}}$ for $q \geqslant 1$. Remarkably, these expressions recover the results obtained in Ref. [49].

We highlight that the self-consistent equations offer a general framework for depicting the equilibrium states. The information about the stationary order parameter R (phase coherence) can be detected from the structures of $F(q)$. For instance, given a fixed value of K, the identity $K^{-1} = F(q)$ determines the roots of q, which, in turn, locate the order parameter R via $q = KR$. In other words, Eq. (46) establishes an implicit function relation between K and R at different C. On that basis, the backward critical coupling corresponding to the desynchronization is marked by the criterion $K_b^{-1} = F(q_b) = \max F(q)$, and the associated critical order parameter is $R_b = q_b F(q_b)$. For example, we have $(K_b, R_b) = (8/\pi, \pi/8)$ for $C = 0$ and $(K_b, R_b) = (2, \sqrt{2}/2)$ for $C = 1$.

Figure 5 illustrates the critical points (K_b, R_b) as a function of C. Upon increasing the correlation factor C, it can be shown that the backward critical point K_b characterizing the termination of synchronized states is decreasing. Meanwhile, the corresponding critical order parameter R_b gets increased. These panels demonstrate that, with the increment of the correlation, the existing region for phase coherence is prolonged accompanied by the overall improved degree of synchronization.

Figure 6 illustrates the order parameters R as the function of C for typical fixed values of $K(K > K_b)$, in which the theoretical predictions and numerical simulations show a prefect agreement. It becomes apparent that the synchronizability can be significantly enhanced by increasing the deterministic correlation, i.e., a larger C leads to a larger order parameter R, provided K is fixed. Actually, the gradual variations of the order parameter and the backward critical points (K_b, R_b) shown in Fig. 5 suggest that a relatively small correlation C is enough to efficiently improve the level of phase coherence. On the basis of the above analyses, we conclude that, even with a given restriction, the proper assignments of the distributed couplings (e.g., introducing deterministic correlations between the couplings and natural frequencies) can greatly facilitate synchronization in coupled oscillator systems.

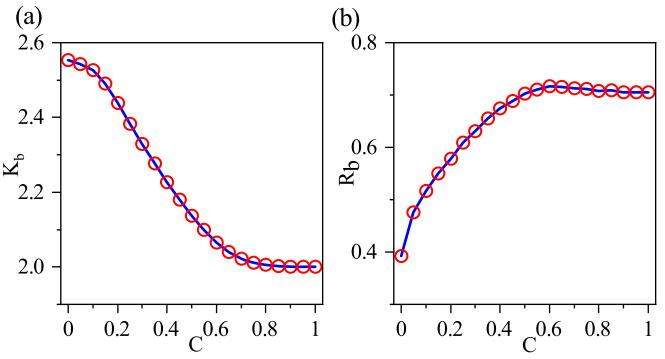

FIG. 5. The backward critical points K_b and R_b for desynchronization transition vs the correlation factor C. In both panels, the solid lines are theoretical predictions from the self-consistent arguments, the circles are numerical simulations with $N = 50\,000$.

V. DISCUSSION

Before concluding, we make brief discussion about the results obtained above. The aim is to clarify how the

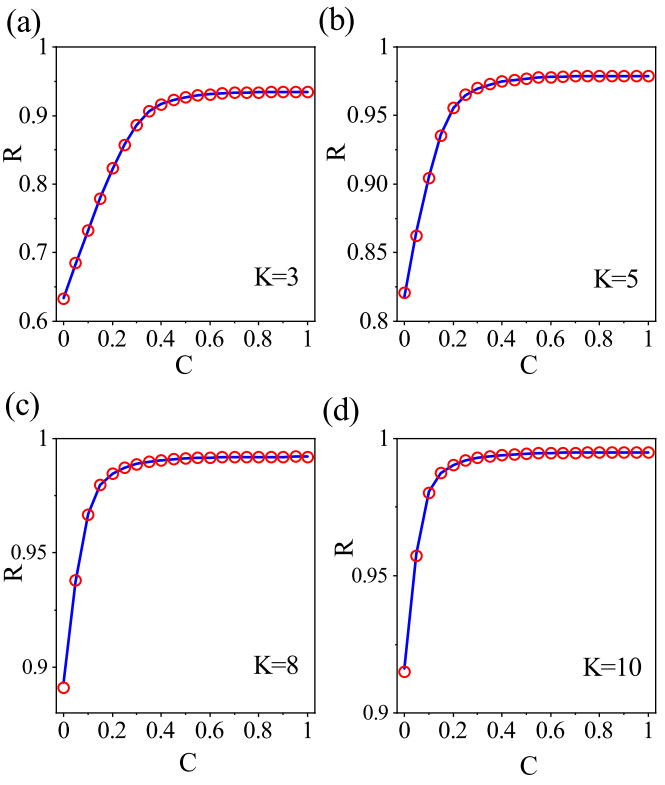

FIG. 6. The order parameter R vs the correlation factor C for typical values of K. The blue solid lines represent the theoretical predictions and the red circles are numerical simulations with $N = 100\,000$.

deterministic-random coupling (DRC) affect the synchronized dynamics in the heterogeneously coupled phase oscillator systems. The main results consist of the following two parts:

In Sec. III, we investigate the impacts of DRC on the forward critical point K_f for the onset of synchronization. Using the linear stability analysis, we obtain the eigenvalue equation describing the instability of the asynchronous state given by Eq. (17). The eigenvalue equation is further discussed in detail in Sec. III B. By imposing critical conditions, the forward critical point K_f is obtained analytically in Eq. (23) that is accompanied by the balanced equation Eq. (24) for the critical frequency Ω. Furthermore, the explicit formulas for the balanced equation are calculated for different cases [Eqs. (25)–(28)].

In Sec. III C, we use the perturbed method to get analytic insights of K_f provided that the correlation factor C is small enough. For this, we introduce the ansatz Eq. (30) with the unknown scaling exponent β and the coefficient Ω_1. Next, the key task is to analyze the perturbed balanced equation Eq. (31) which should be discussed in three different scenarios, respectively, i.e., $0 < \beta < \frac{1}{2}$ [Eq. (35)], $\frac{1}{2} < \beta < 1$ [Eq. (36)], and $\beta = \frac{1}{2}$ [Eq. (37)]. After that, we demonstrate that only the exponent $\beta = \frac{1}{2}$ and the coefficient $\Omega_1 = \pm 1$ are admittable, thereby leading to the scaling behavior of K_f given by Eq. (38).

The results of below synchronization are shown in Figs. 2 and 3 and summarized in Sec. III D. The main conclusion is that the correlation factor has a significant influence on the threshold for synchronization transition. When correlation $C = 0$, the frequency and coupling are totally uncorrelated, at which the critical point corresponding to the onset of synchronization attains the maximum. However, if the deterministic correlation is introduced ($C > 0$), then K_f gets decreased and the deterministic correlation is prone to promote the onset of synchronization. Interestingly, it is found that there exists a critical correlation factor, at which K_f attains the minimum. Finally, for $C^\star(\approx 0.75) < C(\approx 1)$, K_f tends to a constant. Therefore, the overall effect of the deterministic correlation is to render the synchronization transition easier.

Section IV is devoted to untangle the effects of the DRC on the synchronizability above the threshold. We utilize the mean-field argument to obtain the self-consistent equation Eq. (45) through which all the stationary behaviors of the systems can be captured. For convenience, the self-consistent equation Eq. (45) is reformulated as parametric form given by Eq. (46). Subsequently, we focus on discussing the characteristic function $F(q)$ Eq. (47) in various scenarios. The computational processes are tediously complicated and the main steps are as follows:

The first case with $0 \leqslant q < 1$ is discussed in Sec. IV B. Specifically, for $0 \leqslant q < C$, the characteristic function is proven to be undefined. However, for $C \leqslant q < 1$, the characteristic function is summarized as Eq. (58). For the second case $q > 1$ (Sec. IV C), the associated discussions become more involved which should be distinguished with two subcases, respectively. Specifically, in the situation $q \in (1, C^{-1})$, the characteristic function $F(q)$ contains six terms that is summarized in Eq. (77). In the situation $q \in (C^{-1}, \infty)$, the characteristic function $F(q)$ consists of five terms that is listed in Eq. (78). Finally, all the calculation details can be found in the Appendix and the typical results of F(q) are shown in Fig. 4.

The analyses and discussions about the self-consistent equation are conduced in Figs. 5 and 6 and are summarized in Sec. IV D, which mainly involves the dependence of backward critical points and the global order parameter on the correlation factor C. Thus, we conclude that, even with a given restriction, the proper assignments of the distributed couplings (e.g., the deterministic-random correlations) can significantly favor synchronization transition in the networked oscillator systems.

VI. CONCLUSION

In summary, we have investigated the synchronization optimization in the generalized Kuramoto model with deterministic-random coupling (DRC), where the uniformly distributed couplings are rearranged, such that a fraction of which are correlated with the intrinsic frequencies, whereas the remainder retains independent. As reported in the previous studies, it has been identified that the heterogeneous patterns of coupling can shape the collective dynamics of phase oscillators toward synchronization.

Nonetheless, in this work, we uncovered that the appropriate deterministic correlations involved in the DRC can significantly enhance synchronization dynamics. Specifically, we showed that, even within a given restriction, the added deterministic correlations render synchronization transition easier compared to the uncorrelated case. In particular, we revealed that the deterministic correlations have nontrivial impacts on both the onset and vanishing of synchronization. There exists a minimum critical threshold for a certain correlation manifesting the instability of the asynchronous state. Furthermore, we demonstrated that, in the supercritical regime, the increasing deterministic correlations tend to favor synchronization. Both the existing region and the level of phase coherence are remarkably amplified. We developed an analytical treatment to comprehend the essential properties underlying synchronization optimization induced by DRC. Therefore, our work has led a solid foundation for exploring synchronization optimization, and thus provided significant insights for the better understanding of control strategy of synchronization in networked systems.

ACKNOWLEDGMENTS

This work is supported by the National Natural Science Foundation of China (Grants No. 11905068 and No. 11875135), the Natural Science Foundation of Fujian Province, China (Grant No. 2023J01113), and the Scientific Research Funds of Huaqiao University (Grant No. ZQN-810).

APPENDIX: THE DETAILED RESULTS OF THE CHARACTERISTIC FUNCTION

In this Appendix, we list the specific expressions of the characteristic function $F(q)$ in different ranges that are mentioned in the main text.

In the region $1 < q < C^{-1}$ and $C < \alpha q < 1$, the characteristic $F(q)$ in Eq. (70) is

$$F^{q<C^{-1},\alpha q>C}_{q>1,\alpha q<1,(2)} = \frac{1}{q(1-C)}\int_C^{\frac{1}{q}} d\alpha \int_C^{\alpha q} d\omega\sqrt{\Delta} = \frac{U_1 + C(U_2+U_3+U_4+U_5+U_6)}{4(-1+C)q^2}, \quad \text{(A1)}$$

where

$$U_1 = -\arccos C, \quad \text{(A2)}$$
$$U_2 = 3\sqrt{1-C^2}, \quad \text{(A3)}$$
$$U_3 = -3C\sqrt{-1+q^2}, \quad \text{(A4)}$$
$$U_4 = -2C \operatorname{arccsc} q, \quad \text{(A5)}$$
$$U_5 = Cq^2 \operatorname{arcsec} q, \quad \text{(A6)}$$
$$U_6 = 2C \arcsin q. \quad \text{(A7)}$$

In the situation $1 < q < C^{-1}$ and $\alpha q > 1$, the characteristic function $F(q)$ in Eq. (75) is calculated as

$$F^{q<C^{-1}}_{q>1,\alpha q>1,(2)} = \frac{1}{q(1-C)}\int_{\frac{1}{q}}^1 d\alpha \int_C^1 d\omega\sqrt{\Delta} = \frac{\pi + V_1+V_2+V_3+V_4+V_5+V_6+V_7+V_8+V_9}{8(-1+C)q^2}, \quad \text{(A8)}$$

with

$$V_1 = -6C\sqrt{1-C^2}, \quad \text{(A9)}$$
$$V_2 = -6\sqrt{-1+q^2}, \quad \text{(A10)}$$
$$V_3 = 6C\sqrt{-C^2+q^2}, \quad \text{(A11)}$$
$$V_4 = -2q^2 \operatorname{arccsc} q, \quad \text{(A12)}$$
$$V_5 = 4 \operatorname{arcsec} q, \quad \text{(A13)}$$
$$V_6 = -2 \arcsin C, \quad \text{(A14)}$$
$$V_7 = -4C^2 \arcsin C, \quad \text{(A15)}$$
$$V_8 = 2q^2 \arcsin\frac{C}{q}, \quad \text{(A16)}$$
$$V_9 = 4C^2 \arctan\frac{C}{\sqrt{-C^2+q^2}}. \quad \text{(A17)}$$

In the circumstance $q > C^{-1}$ and $\alpha q > 1$, the characteristic function $F(q)$ in Eq. (75) is expressed as

$$F^{q>C^{-1}}_{q>1,\alpha q>1,(2)} = \frac{1}{q(1-C)}\int_C^1 d\alpha \int_C^1 d\omega\sqrt{\Delta} = \frac{W_1+W_2+W_3+W_4+W_5+W_6+W_7+W_8}{4(-1+C)q^2}, \quad \text{(A18)}$$

in which

$$W_1 = -3\sqrt{-1+q^2}, \quad \text{(A19)}$$
$$W_2 = -3C^2\sqrt{-1+q^2}, \quad \text{(A20)}$$
$$W_3 = 3C\sqrt{-C^2+q^2}, \quad \text{(A21)}$$
$$W_4 = 3\sqrt{-1+C^2q^2}, \quad \text{(A22)}$$
$$W_5 = -(1+C^2)(2+q^2)\operatorname{arccsc} q, \quad \text{(A23)}$$
$$W_6 = (2+C^2q^2)\operatorname{arccsc} qC, \quad \text{(A24)}$$
$$W_7 = q^2 \arcsin\frac{C}{q}, \quad \text{(A25)}$$
$$W_8 = 2C^2 \arctan\frac{C}{\sqrt{-C^2+q^2}}. \quad \text{(A26)}$$

[1] S. Boccaletti, V. Latora, Y. Moreno, M. Chavez, and D.-U. Hwang, Complex networks: Structure and dynamics, Phys. Rep. **424**, 175 (2006).

[2] T. Stankovski, T. Pereira, P. V. E. McClintock, and A. Stefanovska, Coupling functions: Universal insights into dynamical interaction mechanisms, Rev. Mod. Phys. **89**, 045001 (2017).

[3] Y. Kuramoto, in *Proceedings of the International Symposium on Mathematical Problems in Theoretical Physics*, edited by H. Araki, Lecture Notes in Physics No. 30 (Springer, New York, 1975), p. 420.

[4] S. H. Strogatz, From Kuramoto to Crawford: Exploring the onset of synchronization in populations of coupled oscillators, Physica D **143**, 1 (2000).

[5] J. A. Acebrón, L. L. Bonilla, C. J. Pérez Vicente, F. Ritort, and R. Spigler, The Kuramoto model: A simple paradigm for synchronization phenomena, Rev. Mod. Phys. **77**, 137 (2005).

[6] A. Pikovsky and M. Rosenblum, Dynamics of globally coupled oscillators: Progress and perspectives, Chaos **25**, 097616 (2015).

[7] T.-W. Ko and G. B. Ermentrout, Partially locked states in coupled oscillators due to inhomogeneous coupling, Phys. Rev. E **78**, 016203 (2008).

[8] E. Montbrió and D. Pazó, Collective synchronization in the presence of reactive coupling and shear diversity, Phys. Rev. E **84**, 046206 (2011).

[9] H. Hong and S. H. Strogatz, Kuramoto model of coupled oscillators with positive and negative coupling parameters: An example of conformist and contrarian oscillators, Phys. Rev. Lett. **106**, 054102 (2011).

[10] D. Iatsenko, S. Petkoski, P. V. E. McClintock, and A. Stefanovska, Stationary and traveling wave states of the Kuramoto model with an arbitrary distribution of frequencies and coupling strengths, Phys. Rev. Lett. **110**, 064101 (2013).

[11] B. Yasmine, Y. Li, W. Jia, and Y. Xu, Synchronization in the network-frustrated coupled oscillator with attractive-repulsive frequencies, Phys. Rev. E **106**, 054212 (2022).

[12] S. Boccaletti, J. A. Almendral, and S. Guan, Explosive transitions in complex networks structure and dynamics: Percolation and synchronization, Phys. Rep. **660**, 1 (2016).

[13] A. R. Francisco, P. Thomas, and K. Juergen, Kuramoto model in complex networks, Phys. Rep. **610**, 1 (2016).
[14] J. Gómez-Gardeñes, S. Gómez, and A. Arenas, Explosive synchronization transitions in scale-free networks, Phys. Rev. Lett. **106**, 128701 (2011).
[15] R. D'Souza, J. Gómez-Gardeñes, and J. Nagler, Explosive phenomena in complex networks, Adv. Phys. **68**, 123 (2019).
[16] C. Xu, H. Yu, and S. Guan, Dynamical origin of the explosive synchronization with partial adaptive coupling, Chaos Solitons Fractals **172**, 113538 (2023).
[17] H. Hong and S. H. Strogatz, Conformists and contrarians in a Kuramoto model with identical natural frequencies, Phys. Rev. E **84**, 046202 (2011).
[18] H. Hong and S. H. Strogatz, Mean-field behavior in coupled oscillators with attractive and repulsive interactions, Phys. Rev. E **85**, 056210 (2012).
[19] S. Petkoski, D. Iatsenko, L. Basnarkov, and A. Stefanovska, Mean-field and mean-ensemble frequencies of a system of coupled oscillators, Phys. Rev. E **87**, 032908 (2013).
[20] D. Iatsenko, P. V. E. McClintock, and A. Stefanovska, Glassy states and super-relaxation in populations of coupled phase oscillators, Nat. Commun. **5**, 4118 (2014).
[21] V. Vlasov, E. E. N. Macau, and A. Pikovsky, Synchronization of oscillators in a Kuramoto-type model with generic coupling, Chaos **24**, 023120 (2014).
[22] I. M. Kloumann, I. M. Lizarraga, and S. H. Strogatz, Phase diagram for the Kuramoto model with van Hemmen interactions, Phys. Rev. E **89**, 012904 (2014).
[23] D. Abrams and S. Strogatz, Chimera states for coupled oscillators, Phys. Rev. Lett. **93**, 174102 (2004).
[24] G. C. Sethia, A. Sen, and F. M. Atay, Clustered chimera states in delay-coupled oscillator systems, Phys. Rev. Lett. **100**, 144102 (2008).
[25] O. E. Omel'chenko, M. Wolfrum, and Y. L. Maistrenko, Chimera states as chaotic spatiotemporal patterns, Phys. Rev. E **81**, 065201(R) (2010).
[26] E. A. Martens, C. R. Laing, and S. H. Strogatz, Solvable model of spiral wave chimeras, Phys. Rev. Lett. **104**, 044101 (2010).
[27] M. J. Panaggio and D. M. Abrams, Chimera states on a flat torus, Phys. Rev. Lett. **110**, 094102 (2013).
[28] Y. Wu, J. Xiao, G. Hu, and M. Zhan, Synchronizing large number of nonidentical oscillators with small coupling, Europhys. Lett. **97**, 40005 (2012).
[29] P. S. Skardal, D. Taylor, and J. Sun, Optimal synchronization of complex networks, Phys. Rev. Lett. **113**, 144101 (2014).
[30] W. Chen, S. Wang, Y. Lan *et al.*, Explosive synchronization caused by optimizing synchrony of coupled phase oscillators on complex networks, Eur. Phys. J. B **94**, 205 (2021).
[31] P. S. Skardal, L. Arola-Fernández, D. Taylor, and A. Arenas, Higher-order interactions can better optimize network synchronization, Phys. Rev. Res. **3**, 043193 (2021).
[32] D. A. Wiley, S. H. Strogatz, and M. Girvan, The size of the sync basin, Chaos **16**, 015103 (2006).
[33] O. E. Omel'chenko, M. Wolfrum, and C. Laing, Partially coherent twisted states in arrays of coupled phase oscillators, Chaos **24**, 023102 (2014).
[34] M. Wolfrum, S. V. Gurevich, and O. E. Omel'chenko, Turbulence in the Ott–Antonsen equation for arrays of coupled phase oscillators, Nonlinearity **29**, 257 (2016).
[35] B. Li and N. Uchida, Large-scale spatiotemporal patterns in a ring of nonlocally coupled oscillators with a repulsive coupling, Phys. Rev. E **104**, 054210 (2021).
[36] A. Yeldesbay, A. Pikovsky, and M. Rosenblum, Chimeralike states in an ensemble of globally coupled oscillators, Phys. Rev. Lett. **112**, 144103 (2014).
[37] E. A. Martens, C. Bick, and M. J. Panaggio, Chimera states in two populations with heterogeneous phase-lag, Chaos **26**, 094819 (2016).
[38] R.-S. Kim, and C.-U. Choe, Symmetry-broken states on a spherical surface of coupled oscillators: From modulated coherence to spot and spiral chimeras, Phys. Rev. E **98**, 042207 (2018).
[39] N. Yao and Z. Zheng, Chimera states in spatiotemporal systems: Theory and applications, Int. J. Mod. Phys. B **30**, 1630002 (2016).
[40] F. Parastesh, S. Jafari, H. Azarnoush, Z. Shahriari, Z. Wang, S. Boccaletti, and M. Perc, Chimeras, Phys. Rep. **898**, 1 (2021).
[41] G. H. Paissan and D. H. Zanette, Synchronization of phase oscillators with heterogeneous coupling: A solvable case, Physica D **237**, 818 (2008).
[42] X. Zhang, X. Hu, J. Kurths, and Z. Liu, Explosive synchronization in a general complex network, Phys. Rev. E **88**, 010802(R) (2013).
[43] I. Leyva, I. Sendiña-Nadal, J. A. Almendral, A. Navas, S. Olmi, and S. Boccaletti, Explosive synchronization in weighted complex networks, Phys. Rev. E **88**, 042808 (2013).
[44] H. Bi, X. Hu and S. Boccaletti, Coexistence of quantized, time dependent, clusters in globally coupled oscillators, Phys. Rev. Lett. **117**, 204101 (2016).
[45] C. Xu, X. Wang, and P. S. Skardal, Generic criterion for explosive synchronization in heterogeneous phase oscillator populations, Phys. Rev. Res. **4**, L032033 (2022).
[46] C. Xu, Y. Zhai, Y. Wu, Z. Zheng, and S. Guan, Enhanced explosive synchronization in heterogeneous oscillator populations with higher-order interactions, Chaos Solitons Fractals **170**, 113343 (2023).
[47] C. Xu, X. Tang, K. Alfaro-Bittner, S. Boccaletti, and S. Guan, Collective dynamics of heterogeneously and nonlinearly coupled phase oscillators, Phys. Rev. Res. **3**, 043004 (2021).
[48] S. H. Strogatz and R. E. Mirollo, Stability of incoherence in a population of coupled oscillators, J. Stat. Phys. **63**, 613 (1991).
[49] C. Xu, Y. Wu, and Z. Zheng, Partial locking in phase-oscillator populations with heterogenous coupling, Chaos **32**, 063106 (2022).